Half-Bridge Series Resonant Inverter for Induction Heating Applications with Load-Adaptive PFM Control Strategy

Young-Sup Kwon, Sang-Bong Yoo, Dong-Seok Hyun

Dept. of Electrical Engineering, Hanyang University
Seongdong-ku, Seoul, 133-791 Korea
Phone : +82-2-290-0341 Fax : +82-2-297-1569
E-mail : dshyun@hyunp1.hanyang.ac.kr

Abstract - **This paper presents an effective control scheme incorporated in the voltage-fed half-bridge series resonant inverter for induction heating applications, which is based upon a load-adaptive tuned frequency tracking control strategy using PLL(Phase Locked Loop) and its peripheral control circuit. The proposed control strategy ensures a stable operation characteristics of overall inverter system and ZVS(Zero Voltage Switching) operation in spite of sensitive load parameters variation as well as power regulation, specially in the non-magnetic heating loads. The operation principle and the design procedure of the inverter system with the proposed control scheme are described. Also, the simulation results and the performance characteristics in the steady-state are shown as compared with the experimental results for a prototype induction cooking system rated at 1.2*kW.**

I. INTRODUCTION

In recent years, with remarkable advancements of power semiconductor devices and electronic control systems, much attention has been focused on the research and developments of high-frequency resonant inverters capable of supplying high-power to induction heating loads. The various resonant inverters using MOSFETs, IGBTs, MCTs, SITs offer reduced power device switching losses by means of soft-switching technique and attractive possibilities in developing higher frequency of operation, higher efficiency, lightweight and overall system simplicity in terms of inverter control, protection and maintainability [1]-[5].

The induction cooking is one of the many applications for induction heating using high-frequency resonant inverters. It is designed to replace ordinary stove plates. Although induction cooking has high initial cost in comparison with a conventional stove plate, it has many advantages including cleanness, safety, high efficiency, high power density, high reliability, maintainability and controllability [6], [7].

However, in spite of these many advantages, conventional induction cooking systems have been designed to operate with cooking vessel made from a specific material, mainly cast iron of ferro-magnetic stainless steel, which has a high resistivity and relative permeability. Besides, it is difficult to heat non-magnetic materials such as aluminum vessels often used for general household applications due to following reasons [7], [8];

- Low resistivity and relative permeability
- Parameter variation is more sensitive than that of magnetic materials
- Sensitive power control characteristics

These reasons cause overall inverter system to operate unstably under constant frequency control because the performance of inverter is highly effected upon characteristics of load parameters. Therefore, the inverter system with a load-adaptive control circuit is required to operate successfully irrespective of variation of the load parameters. In this paper, an effective control scheme incorporated in the voltage-fed half-bridge series resonant inverter for induction heating applications is presented, which is based upon a load-adaptive tuned frequency tracking control strategy using PLL(Phase Locked Loop) and its peripheral control circuit. The proposed control scheme can ensure reliability of overall inverter system and operation under the principle of ZVS(Zero Voltage Switching) in spite of power regulation process as well as load fluctuations, specially in non-magnetic heating loads. In this inverter system, output power regulation is based upon PFM(Pulse Frequency Modulation) through phase-shifting angle. Furthermore, the operation principle and the design procedure of the inverter system with the proposed control scheme are described and its performance characteristics in steady state are verified by the simulation and experimental results for a prototype induction cooking system rated at 1.2*k*W.

II. PRINCIPLE OF INDUCTION HEATING AND ANALYSIS OF LOAD CHARACTERISTICS

A. Principle of Induction Heating

Induction heating is the principle that the magnetic field induced in the coil when energized, causes eddy currents to occur in the heating load and these give rise to the heating effect, as shown in Fig. 1. The most of the heat, generated by eddy currents in the heating load is concentrated in a peripheral layer of skin depth δ given by;

$$\delta = \sqrt{\frac{1}{4\pi^2 \times 10^{-7}}} \cdot \sqrt{\frac{\rho}{\mu_r f}} \qquad (1)$$

0-7803-5160-6/99/$10.00 © 1999 IEEE.

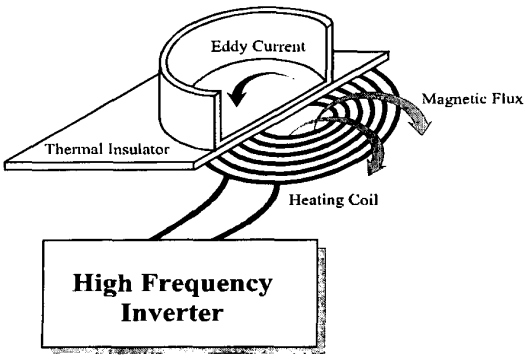

Fig. 1. Principle of induction heating.

Where μ_r and ρ are relative magnetic permeability and electrical resistivity of the material, respectively and f is operating frequency. It is also important factor to determine operating frequency for induction heating applications.

B. Equivalent Circuit and Analysis of Load Characteristics

In general, the heating coil and the load are modeled as a transformer with a single turn secondary winding. As shown in Fig. 2, the equivalent model for a transformer can be represented in a simplified form by an equivalent inductance and resistance. These load parameters depend on several variables including the shape of the heating coil, the spacing between the heating coil and cooking vessel, their electrical conductivity and magnetic permeability, and the operating frequency. So, it is necessary for analyzing load characteristics for the induction heating system. The heating coil and the load can be represented by an equivalent series inductance L_{eq} and resistance R_{eq} as given by;

$$L_{eq} = L_1 - \frac{(\omega M)^2 \cdot L_2}{R_L^2 + (\omega L_2)^2} = L_1 - A^2 \cdot L_2 \qquad (2)$$

$$R_{eq} = r + \frac{(\omega M)^2 \cdot R_L}{R_L^2 + (\omega L_2)^2} = r + A^2 \cdot R_L \qquad (3)$$

$$Where\ A = \frac{\omega M}{\sqrt{R_L^2 + (\omega L_2)^2}} \approx \frac{M}{L_2} \quad at\ \omega L_2 \rangle\rangle R_L$$

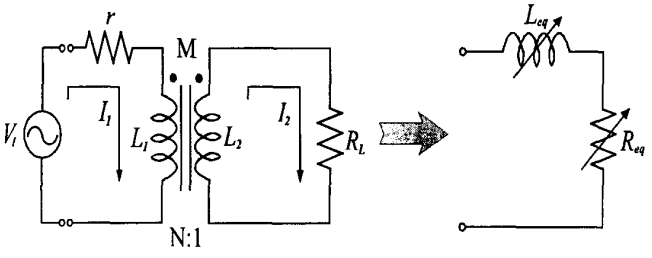

Fig. 2. Equivalent circuit for a transformer.

TABLE I
ELECRTRICAL CHARACTERISTICS

Parameter	*Iron*	*Aluminum*
Resistivity	9.8×10^{-8}	2.5×10^{-8}
Relative permeability	*100*	*1*
Skin depth	*0.11*	*0.56*
Surface resistance	8.8×10^{-4}	0.45×10^{-4}

Also, since secondary resistance R_L can be determined by skin depth of eddy current, actual output power is represented by relation of resistance and current as given by;

$$R_L = \frac{\rho}{\delta} = k\sqrt{\rho\mu_r f} \quad and \quad I_2 = NI_1 \qquad (4)$$

$$P = k \cdot (NI_1)^2 \cdot \sqrt{\rho\mu_r f} \qquad (5)$$

Where k : constant(0.0019869), N : turn numbers of heating coil

Table I shows electrical characteristics according to materials at 20*k*Hz. It is known that non-magnetic materials such as aluminum have much lower resistivity and permeability in comparison with magnetic materials as iron. Therefore, the increase of output power when heating load is non-magnetic material requires the following conditions from expression (5);

- Increase of current frequency in heating coil
- Increase of Ampere-Turn(N)

However, the increase of frequency and turn numbers for heating non-magnetic loads, it results in characteristics of output power more sensitive compared with that of magnetic load as shown in Fig. 3. In addition to, the skin and proximity effects cause the winding parasitic resistance of an inductor to increase with the operating frequency and effect on the overall efficiency of the induction heating system.

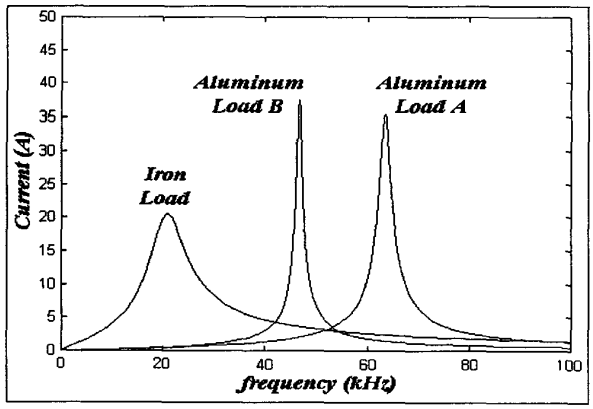

Fig. 3. Output current characteristics according to materials.

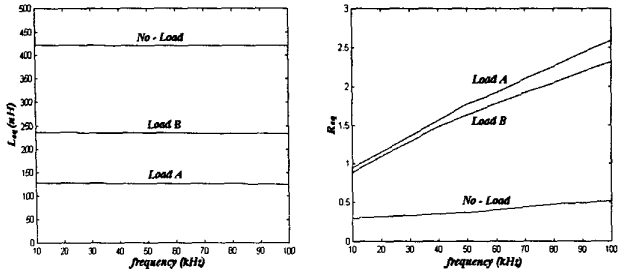

(a) Variation of L_{eq} and R_{eq} according to frequency

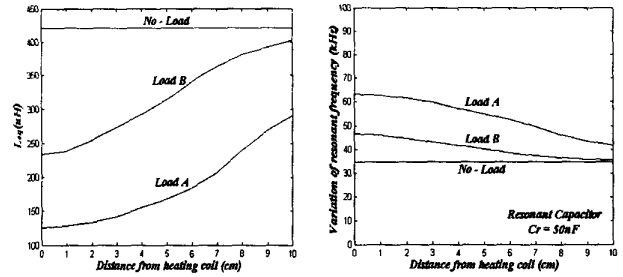

(b) Variation of L_{eq} and f_r according to distance of loads from the center of the heating coil

Fig. 4. Parameters variation for load condition.

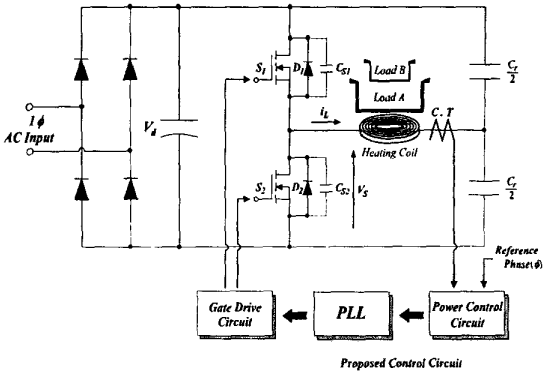

(a) Overall inverter system configuration

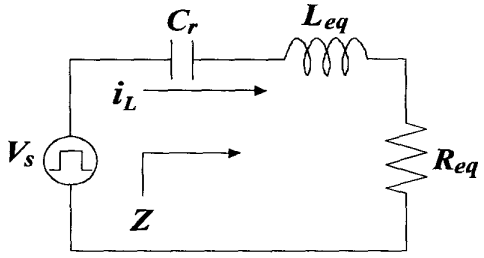

(b) Equivalent circuit

Fig. 5. Configuration of induction cooking system.

In order to evaluate the characteristics of parameter variation, the aluminum vessels which is one of the non-magnetic materials were tested as the heating load. The load A and the load B are aluminum vessels diameter of $22cm$ and $10cm$, respectively. Fig. 4(a) shows variation of the equivalent parameters L_{eq} and R_{eq} according to the switching frequency and loads.

Also, it is noted that equivalent inductance L_{eq} and resonant frequency f_r are sensitively varied according to loads and the distance between the heating coil and loads from the center of the heating coil, as shown in Fig. 4(b).

III. System Configuration and Operation

Fig. 5 shows a system configuration of induction cooking system and its equivalent circuit. The voltage-fed half-bridge series resonant inverter consists of two switches S_1, S_2 using MOSFETs, which are alternately on and off with a duty ratio of 50%, and two resonant capacitors $C_r/2$ and the equivalent inductance L_{eq} and resistance R_{eq}, which represent the heating coil and load. The lossless snubbing circuit consisting of only a capacitor is connected between the drain and source of each MOSFET. Also, it includes the proposed control block for ensuring a stable operation of inverter system. One of the main advantages of the half-bridge inverter is low voltage across the switches that is equal to the supply voltage. Thus, compared with other topologies(Class-E, Quasi-resonant inverter etc.) for induction heating applications, it is suited for high-voltage applications [9], [10].

Fig. 6 describes the operation mode including switching signals and inverter output voltage V_S and current i_L waveforms. As shown in Fig. 6, if the switches are operated above resonant frequency, the series resonant circuit represents an inductive load and the load current i_L lags behind the output voltage V_S. Therefore, load current i_L flows in the order of $C_{S1},C_{S2} \rightarrow D_1 \rightarrow S_1 \rightarrow C_{S1},C_{S2} \rightarrow D_2 \rightarrow S_2$. At this time, the switching losses are not occurred at turn-on because the switches are turned on at zero voltage i.e. ZVS(Zero Voltage Switching).

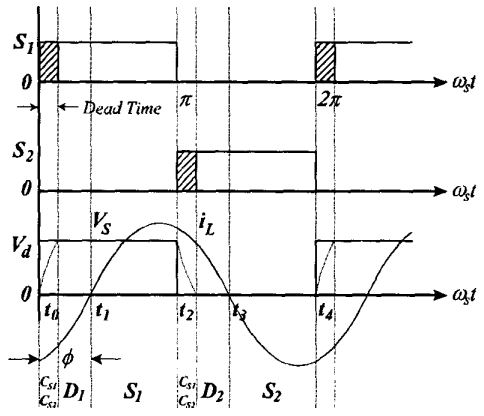

Fig. 6. Operation mode of half-bridge inverter.

IV. PROPOSED CONTROL STRATEGY

A. Power Regulation Scheme

In general, output power regulation scheme can be classified into two large ways in the half-bridge resonant inverter. The first method, so called PAM(Pulse Amplitude Modulation), is to adjust the DC power supply voltage by means of the thyristorized phase-controlled rectifier or the chopper. The second power control method is to vary operating frequency on the basis of PFM(Pulse Frequency Modulation) strategy. Compared with PAM control, PFM control scheme is preferred in the half-bridge resonant inverter because it has the advantage with respect to volumetric size and operating technique, no requiring any controlled power converter in DC link voltage. As a result, the line harmonic noises in the utility-grid are relatively low and a fast control response and more cost-effective system is expected to be obtained. Therefore, in this inverter system, output power regulation is based upon PFM method through phase-shifting angle ϕ. As shown in Fig. 6, assuming that the input voltage V_S of the resonant tank circuit is regarded as a square wave and quality factor Q is so high as to the load current i_L through the resonant tank circuit is sinusoidal. Output power can be derived as follows;

The input impedance of the resonant tank circuit and the current angle can be represented by expression (6) and (7).

$$Z = R_{eq} + j\left(\omega_s \cdot L_{eq} - \frac{1}{\omega_s \cdot C_r}\right)$$

$$= R_{eq} \cdot \sqrt{1 + Q^2 \cdot \left(\omega_n - \frac{1}{\omega_n}\right)^2} \angle\phi \qquad (6)$$

$$\phi = \tan^{-1}\left(Q \cdot \left(\omega_n - \frac{1}{\omega_n}\right)\right) \qquad (7)$$

$$Where \quad \omega_r = \frac{1}{\sqrt{L_{eq} \cdot C_r}}, \quad \omega_n = \frac{\omega_s}{\omega_r}, \quad Q = \frac{\omega_r \cdot L_{eq}}{R_{eq}}$$

The fundamental wave of input voltage V_S of the resonant tank circuit can be found from Fourier analysis as follows;

$$V_{S1} = \frac{2 \cdot V_D}{\pi} \cdot \sin \omega_s t \qquad for \quad 0 < \omega_s t \le 2\pi \qquad (8)$$

The load current through the resonant tank circuit can be expressed as

$$i_L = I_m \cdot \sin(\omega_s t - \phi) = \frac{2 \cdot V_D \cdot \cos\phi}{\pi \cdot R_{eq}} \cdot \sin(\omega_s t - \phi) \qquad (9)$$

Therefore, the output power is given by using expression (9)

$$P_{out} = \frac{{I_m}^2 \cdot R_{eq}}{2} = \frac{2 \cdot {V_D}^2 \cdot \cos^2\phi}{\pi^2 \cdot R_{eq}} \qquad (10)$$

B. Frequency Tuning Control Scheme

The heating coil and the load can be modeled by means of a series combination of its equivalent resistance R_{eq} and inductance L_{eq}. Specially in the proposed inverter system, these parameters depend on several variables as above-mentioned. Therefore, it becomes necessary to vary operating frequency of the inverter in order to maintain its constant output power irrespective of load variations. This implies that the inverter switching frequency must vary during operation, depending on the resonant frequency of the inverter circuit.

Fig. 7 shows the overall control block diagram and its key waveforms including PLL and its peripheral circuit to accomplish above performance. The used CMOS type PLL(CD4046) plays a major role in the inverter operation. The proposed control circuit and its detail operation is explained as follows;

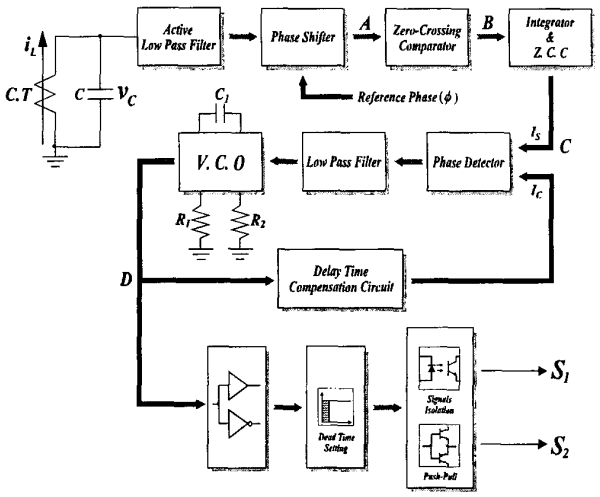

(a) Overall control block diagram

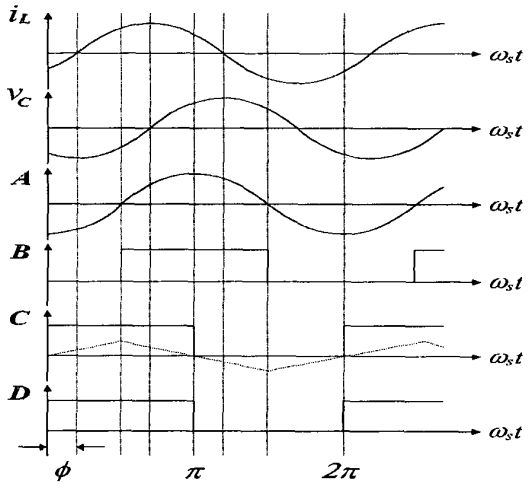

(b) Key waveforms

Fig. 7. Proposed load-adaptive control scheme.

Isolated output current in inverter circuit is derived from high-frequency current transformer (C.T) as a sensor and current conversion ratio is set to a specific value. This detected current signal is converted into the voltage signal V_C by the capacitor C, and at the same time, the phase angle lags to be 90°. However, the detected current signal is subject to switching noise due to commutation of switches. Therefore, its signal is filtered by active low pass filter and fed to phase shifter in order to output power control. The shifted signal as ϕ is converted to square wave signal by zero crossing comparator and then becomes a 90° leading square wave signal by integrator and zero crossing comparator for compensating 90° lagging current signal. This current signal is input I_S of PLL and equal to phase of inverter output voltage at the same time. The used PD(Phase Detector) in this system is a positive edge controlled logic circuit consisting essentially of four flip-flops and a pair of MOS transistors. When the frequency of I_S and I_C signals are unequal, PD gives an output signal indicating frequency difference, and when locked it indicates a phase difference. The PD output signal is used to shift the VCO toward lock before capture, then holds the frequency in lock as in a conventional PLL circuit. Locked condition is obtained when both I_S and I_C signals have equal frequency with their phase difference equal to zero. The VCO produces an output signal whose frequency is determined by the input DC voltage from external low pass filter and the connected resistors and capacitor. In general, VCO output signal is directly feedback to I_C and fed to the gate drive circuit. But a specific delay time is occurred in filter and the gate drive circuit and so on. In order to compensate this delay time, VCO output signal is fed to delay time compensation circuit and then compared with signal I_S. The switches S_1, S_2 are driven by VCO output signals with dead time through isolation and push-pull circuit.

V. Simulation and Experimental Results

The validity of the proposed load-adaptive control circuit was verified by the simulation and experimental results for a prototype induction cooking system. The half-bridge resonant inverter was built using MITSUBISHI MOSFET FM50DZ-10S (500V/50A) as main switching devices. The aluminum vessels, which is one of the non-magnetic materials were tested as the heating load, as analyzed in section II. Litz wire of 65 turns was used for heating coil in order to reduce the losses due to skin and proximity effects, and it is coiled in a flat spiral form and forced air cooled. The spacing between cooking vessel and the heating coil was maintained 4mm thickness using thermal insulator. The system parameter is followed as; V_D=100V, C_r=50nF, C_{S1}=C_{S2}=10nF, *Dead Time*=1.1us. And the parameters according to loads are shown in Table II.

TABLE II
PARAMETERS ACCORDING TO LOADS

Parameter	*Load A*	*Load B*	*No-Load*
L_{eq}	*126 uH*	*233 uH*	*421 uH*
R_{eq}	*1.8 Ω*	*1.7 Ω*	*0.4 Ω*
F_r	*63.4 kHz*	*46.6 kHz*	*34.6 kHz*

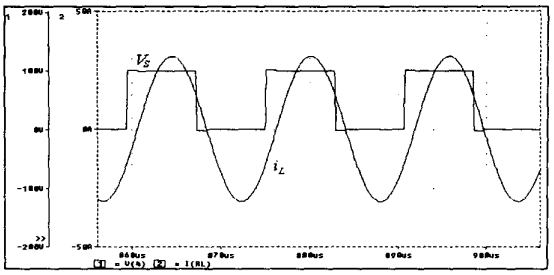

(a) Load B → Load A

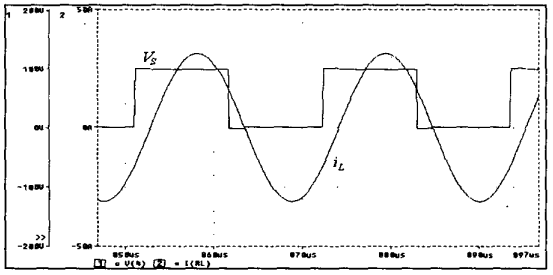

(b) Load B

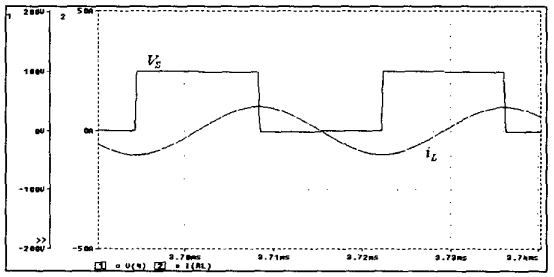

(c) Load B → No Load

Fig. 8. Simulation waveforms of V_S and i_L for the reference phase ϕ = 30°.

Fig. 8 and 9 show the simulation and experimental results of inverter system with the proposed load-adaptive control strategy for the reference phase ϕ = 30°, respectively. From Fig. 9, the experimental results show a good agreement with those of the simulation, as shown in Fig. 8. It is noted that operating frequency of inverter is adaptively varied so as inverter to operate stably under ZVS condition for each load. In case of no-load, it results from setting the minimum operating frequency of PLL as 36kHz. Otherwise, high load current flows in inverter system due to low equivalent resistance.

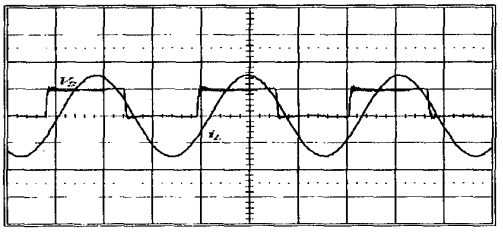

(a) Load B → Load A

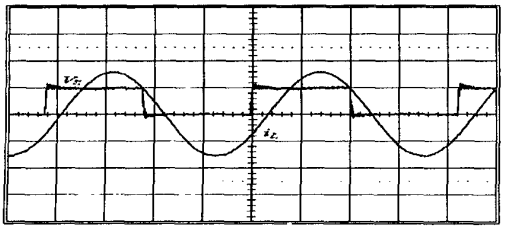

(b) Load B

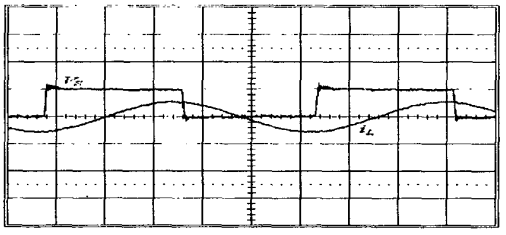

(c) Load B → No Load

Fig. 9. Experimental waveforms of V_S and i_L for the reference phase $\phi = 30°$. (100V/div., 20A/div., 5*us*/div.)

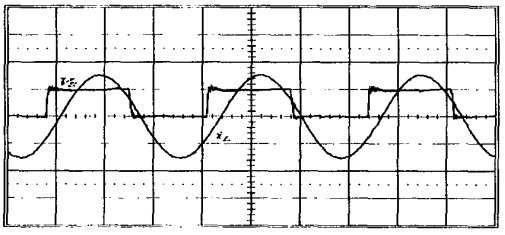

(a) Load A

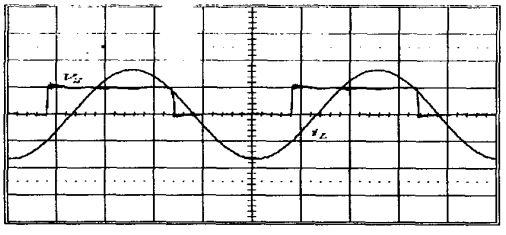

(b) Load B

Fig. 10. Experimental waveforms of V_S and i_L for the moved loads of 3*cm* distance. (100V/div., 20A/div., 5*us*/div.)

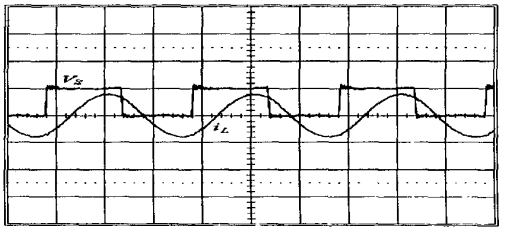

(a) Load A

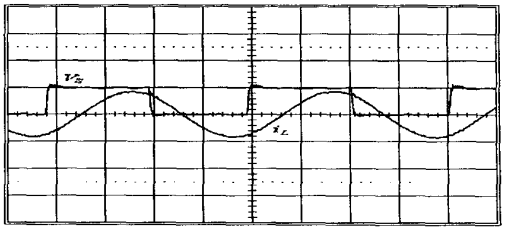

(b) Load B

Fig. 11. Experimental waveforms of V_S and i_L for the reference phase $\phi = 60°$. (100V/div., 20A/div., 5*us*/div.)

Fig. 10 shows the experimental results when each load is moved from the center of the heating coil as 3*cm* distance. Fig. 11 shows experimental results for the reference phase ϕ = 60°. Likewise, with the help of the proposed control circuit, inverter system achieves a stable operation by tracking operation frequency for load A and load B, respectively.

From above the results, it is confirmed that the proposed control scheme can ensure reliability of overall inverter system in spite of power regulation as well as load fluctuations.

VI. CONCLUSION

In this paper, an effective control scheme incorporated in the voltage-fed half-bridge series resonant inverter for induction heating applications has been proposed, which is based upon a load-adaptive tuned frequency tracking scheme characterized through PLL control and its peripheral interface implementations. Besides, the operation principle of the inverter system with the proposed control scheme has been demonstrated and its performance characteristics in the steady-state have been verified by the simulation and experimental results for a prototype induction cooking system. The main advantages of this inverter system are characterized as follows;

- Applicable to non-magnetic load such as aluminum as well as magnetic load
- Effective operation under ZVS condition irrespective of largely-changed load parameters as well as power regulation based upon PFM strategy
- The reduction in size and weight
- Wide power regulation range

Therefore, the proposed control strategy can ensure reliability of the inverter system and be expected to be effectively applied to different induction heating applications.

REFERENCES

[1] S. Bottari, L. Malesani, and P. Tenti, "High-Efficiency 200kHz Inverter for Induction Heating Appliance", *IEEE-PESC Conf. Rec.*, pp. 308-316, 1985.

[2] S. Nagai, H. Nagura, A. Okuno, and M. Nakaoka, "High-Frequency Inverter with Phase-Shifted PWM and Load-Adaptive PFM Control Strategy for Industrial Induction-Heating", *IEEE-IAS Conf. Rec.*, Vol. 3, pp. 2165-2172, 1993.

[3] A. Okuno, M. Hayashi, H. Kawano, and M. Nakaoka, "Practical Evaluations of Load-Adaptive High-Frequency Resonant PAM Inverter Using Static Induction Power Transistors for Industrial Induction-Heating Plants", *IEEE-IECON Conf. Rec.*, Vol. 2, pp. 1015-1020, 1993.

[4] M. Kamli, S. Yamamoto, and M. Abe, "A 50-150kHz Half-Bridge Inverter for Induction Heating Applications", *IEEE Trans. on Industrial Electronics*, Vol. 43, No. 1, pp. 163-172, 1996.

[5] H. Fujita, and H. Akagi, "Pulse-Density-Modulated Power Control of a 4kW, 450kHz Voltage-Source Inverter for Induction Melting Applications", *IEEE Trans. on Industry Applications*, Vol. 32, No. 2, pp. 297-286, 1996.

[6] S. P. Wang, M. Nakaoka, K. Izaki, I. Hirota, H. Yamashita, and H. Omori, "Soft-Switched PWM High-Frequency Load-Resonant Inverter with Power Factor Correction for Induction Heating Cooking Appliance", *EPE Conf. Rec.*, Vol. 2, pp. 244-249, 1997.

[7] Henry W. Koertzen, Jacobus D. van Wyk, and Jan A. Ferreira, "Design of the Half-Bridge, Series Resonant Converter for Induction Cooking", *IEEE-PESC Conf. Rec.*, pp. 729-735, 1995.

[8] J. W. Jung, B. K. Lee, B. S. Suh, and D. S. Hyun, "A New Half-Bridge Inverter Topology with Active Auxiliary Resonant Circuit Using Insulated Gate Bipolar Transistors for Induction Heating Applications", *IEEE-PESC Conf. Rec.*, Vol. 2, pp. 1232-1237, 1997.

[9] M. K. Kazimierczuk, "Class-D Voltage-Switching MOSFET Power Amplifier", *IEE-Proc.*, Vol. 138, No. 6, pp. 285-296, 1991.

[10] J. Ying, and K. Heumann, "Design and Application of Class E Amplifier", *IEEE-IPEC Conf. Rec.*, pp. 1191-1196, 1995.